PHYSICAL REVIEW B VOLUME 31, NUMBER 9 1 MAY 1985

Itinerant-electron antiferromagnetism and superconductivity in bcc Cr-Re alloys

Y. Nishihara and Y. Yamaguchi
Electrotechnical Laboratory, Sakura-mura, Ibaraki 305, Japan

T. Kohara
College of Liberal Arts, Kobe University, Kobe 657, Japan

M. Tokumoto
Electrotechnical Laboratory, Sakura-mura, Ibaraki 305, Japan
(Received 4 December 1984)

The magnetic and superconducting properties of bcc Cr-Re alloys with up to 40 at. % Re were studied via measurements of the magnetic susceptibility, electrical resistivity, and nuclear magnetic resonance of the Re nuclei. Antiferromagnetic order coexists with superconductivity above 18 at. % Re. The results were analyzed with the coexistence model of spin-density waves and superconductivity. In the Re-concentration range greater than 18 at. %, about 10% of the Fermi surface satisfies the nesting condition and the rest of it contributes to form the superconducting gap. This model also explains the increase in the superconducting transition temperature and the decrease in the magnetic susceptibility by annealing as a competing effect between spin-density waves and superconductivity.

I. INTRODUCTION

The interplay between magnetism and superconductivity has been studied by theoreticians and experimentalists for more than two decades. Long-range magnetic order has been observed, together with superconductivity, in some ternary rare-earth (R) compounds, such as, $R_x Mo_6S_8$ and RRh_4B_4. In these compounds the magnetic moment is carried by localized $4f$ electrons on R atoms and couples weakly with superconducting $4d$ electrons on Mo or Rh atoms. Intensive researches revealed that an antiferromagnetic or spiral state coexists with superconductivity in these systems.[1]

When the magnetic state is an itinerant-electron type, the interaction between magnetic and superconducting electrons is thought to be strong compared with that in the above systems. Therefore, it is expected that the coexistence of magnetic order and superconductivity is hard to realize. Recently, however, it has been found[2] that the intermetallic compound Y_9Co_7 shows ferromagnetism and superconductivity. The magnetic properties of this compound are those of a very weak itinerant-electron ferromagnet.[3] On the other hand, the superconducting properties are those of an inhomogeneous superconductor with a spatially varing critical current.[4] We think this material is suitable for investigating the interplay between superconductivity and itinerant-electron ferromagnetism.

Chromium metal is known as a typical itinerant-electron antiferromagnet. The CrRe system has the bcc structure up to ~ 50 at. % Re.[5] In the Re-concentration region greater than ~ 35 at. %, the low-temperature phase is a mixture of the α and σ phases. The σ phase has a tetragonal structure. At 40 at. % Re, the pure α phase is obtained when the alloy is quenched from over 1800 °C. Muheim and Müller[6] observed superconductivity in the Re-concentration region greater than 18 at. %. They concluded that the coexistence or antiferromagnetism and superconductivity was rather improbable, because the magnetic ordering temperature estimated from the temperature dependence of resistivity disappears at about 16 at. % Re. After that, the spin-density-wave (SDW) behavior of the bcc CrRe system was studied by many workers.[7–12] The Néel temperature of this system increases with increasing Re concentration up to ~ 5 at. % and decreases above ~ 10 at. %.[7,8] On the other hand, the magnetic moment increases up to ~ 3 at. % Re and then decreases with increasing Re concentration. The incommensurate SDW changes into a commensurate SDW at ~ 0.78 at. % Re.[9,10] There was no report on magnetic properties in the Re-concentration region greater than 18 at. %.

Recently, we have studied the magnetic properties of the bcc CrRe system and found that this system exhibits magnetic order even in the Re-concentration region greater than 18 at. % Re.[13,14] Theoretically, it is thought that the SDW coexists with superconductivity by shearing the Fermi surface.[15] The competition between SDW behavior and superconductivity has been extensively studied in organic superconducting systems.[16] However, the coexistence of SDW behavior and superconductivity has not been found in these systems. Therefore, the bcc CrRe system will provide useful information on the interplay between itinerant-electron antiferromagnetism and superconductivity. This paper gives experimental results on the magnetic and superconducting properties of bcc Cr-Re alloys. The results are discussed by using the theory[15] of the coexistence of SDW's and superconductivity.

II. EXPERIMENTAL RESULTS

A. Superconducting properties

Alloys of $Cr_{100-x}Re_x$ were prepared by the arc melting of Cr and Re metals with 99.99% purities. X-ray diffraction gave the bcc pattern without extra phases. The lattice constant of the unannealed alloy increases linearly with increasing Re concentration as shown in Fig. 1.

Figure 2 shows the superconducting transition temperature T_c of the unannealed alloy (defined at the midpoint of the change in resistivity) and the electronic specific-heat coefficient γ plotted against the Re concentration. The γ values are those reported by Muheim and Müller.[6] Superconductivity is observed in the samples with $x \geqq 18$. The transition temperature increases with increasing x up to 20. The increasing rate becomes small between $x=20$ and 30, and again rapidly increases above $x=30$. On the other hand, the change in γ shows only one step increase. It starts to increase at $x \sim 12$ and saturates at ~ 26. The Debye temperatures are 410—460 K for the alloys with $x \geqq 10$.[6] Although the σ phase is not observed by x-ray diffraction, a small amount of the σ phase might be present in the samples with $x > 30$. However, since the T_c of the σ phase is about 2 K,[6] the increase in T_c for $x > 30$ cannot be attributed to the presence of the σ phase.

The temperature dependence of the upper critical field H_{C2} is shown in Fig. 3. H_{C2} was determined from the midpoint of the resistivity change. The temperature dependence with a positive curvature for $x > 30$ could originate from an inhomogeneity of the superconducting properties due to the large change in the transition temperature above $x=30$.

B. Magnetic properties

Figure 4 shows the temperature dependence of the magnetic susceptibility of the unannealed samples with $x \geqq 20$. The value of the susceptibility decreases with increasing Re concentration. The susceptibility shows a peak around 160 K in the samples with $x \leqq 30$. The position of the peak is almost independent of Re concentration within ± 10 K. The peak becomes obscure for the sample with

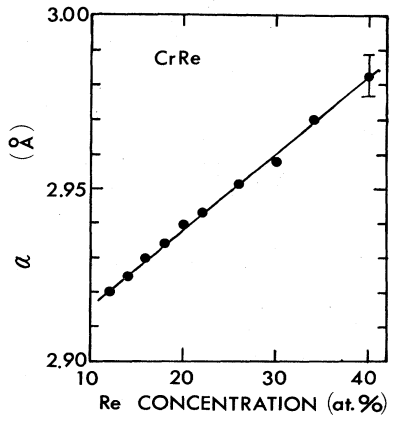

FIG. 1. Lattice constant of bcc Cr-Re alloys.

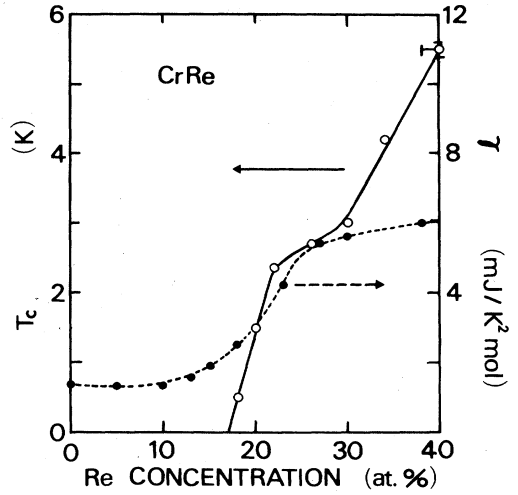

FIG. 2. Superconducting transition temperature T_c and the electronic specific-heat coefficient γ of bcc Cr-Re alloys. The values of γ are those from Ref. 6.

$x=40$. The magnetization curve was linear up to 40 kOe at 4.2 K. The initial magnetization of $x=26$ exhibits perfect diamagnetism below ~ 100 Oe ($=H_{C1}$) at 0.5 K. The temperature dependence of the susceptibility suggests that antiferromagnetic order exists even in the alloy with $x \geqq 20$. In order to make clear the presence of magnetic order below the peak of the susceptibility, we made nuclear magnetic resonance (NMR) measurements of Re.

Another series of alloys was annealed at 1050°C for 1 week and then crushed into powder for the NMR measurements. The average particle size as measured by an optical microscope was about 20 μm. The superconducting transition temperatures of these powdered samples were 3.1 K for $x=26$ and 3.4 K for $x=30$. The NMR spectrum was measured with a variable-frequency spin-

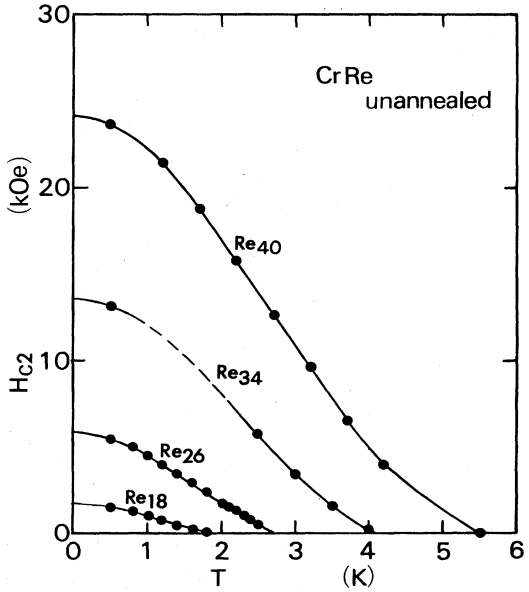

FIG. 3. Temperature dependence of H_{C2} of bcc Cr-Re alloys.

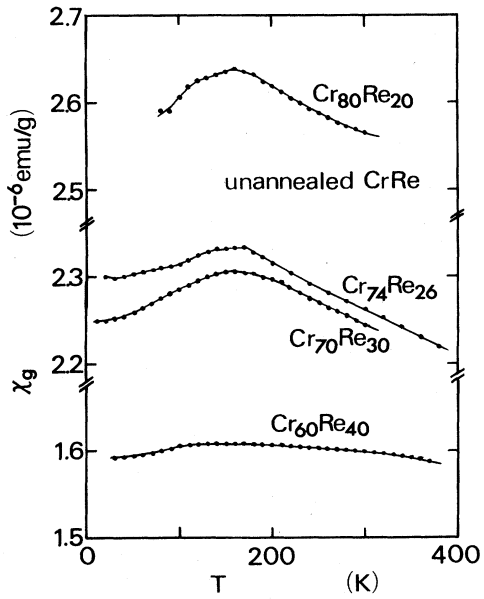

FIG. 4. Temperature dependence of the susceptibility of bcc Cr-Re alloys.

echo spectrometer. The spin-echo spectrum of ^{185}Re and ^{187}Re in the sample with $x=26$ in an external field of 3 kOe at 1.3 K is shown in the upper half of Fig. 5. Since the sample is in the superconducting state at 1.3 K, the NMR intensity is very weak in zero external field. To obtain a good signal-to-noise ratio, the measurement was made in an external field of 3 kOe, where the sample is in the mixed state. The shape of the spectrum agrees with that in zero external field at 4.2 K. The spectrum has a peak around 55 MHz. Since ^{185}Re and ^{187}Re nuclei have nuclear spins of $I=\frac{5}{2}$, if the signal comes from the pure electric quadrupole effect, a similar signal should appear in the frequency region of twice or half of the observed signal. No signal was observed in the above frequency region, so we can conclude that the NMR signal arises from the magnetic hyperfine interaction. The peak position of the spectrum corresponds to a hyperfine field of ~ 52 kOe. Since no enhancement effect of the NMR signal, which is a characteristic of ferromagnets, was observed and the magnetization curve is linear up to 40 kOe, the magnetic order is antiferromagnetic in Cr-Re alloys with $x \geqq 20$.

The lower part of Fig. 5 shows the external field dependence of the NMR signal at 40 MHz. The solid curve ρ in the figure represents the relative change in the electrical resistivity at 1.3 K. The NMR intensity rapidly increases above $H_{C2}=3.2$ kOe and becomes 50 to 60 times as large as that at zero external field. The NMR signal in the superconducting state comes from the spins in the London penetration depth. The intensity change from the superconducting to the normal state can be quantitatively explained taking into account the average particle size of ~ 20 μm and the penetration depth of ~ 1000 Å which is a typical value of type-II superconductors. The result shows that the magnetic hyperfine field exists at Re nuclei in the superconducting state.

The nuclear spin-lattice relaxation time T_1 provides information about the electronic states at the Fermi level. Figure 6 shows the temperature dependence of the nuclear spin-lattice relaxation rate $1/T_1$ for the sample with $x=26$ in external fields of 2 and 7 kOe. When we apply an external field which is larger than H_{C2}, T_1 follows the Korringa relation ($T_1T=$ const). In the superconducting state (at temperatures below T_c and in the external field below H_{C2}) the values of T_1 increases exponentially with decreasing temperature in samples both with $x=26$ and $x=30$. The superconducting energy gap estimated from the temperature dependence of T_1 is 1.4—$1.6k_BT_c$ and a little smaller than the BCS value of $1.76k_BT_c$. The result shows that T_1 becomes longer in the superconducting state because of the appearance of the energy gap.

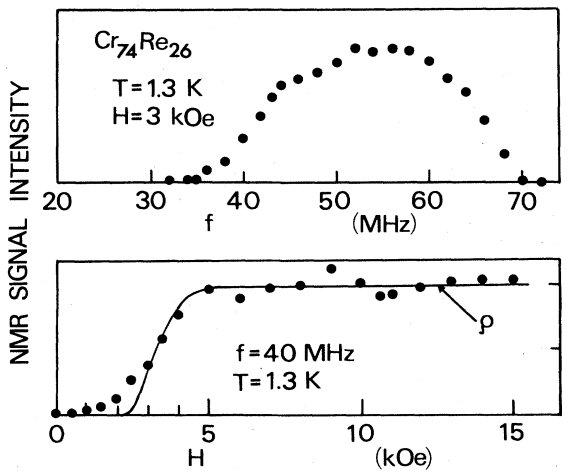

FIG. 5. Nuclear magnetic resonance spectrum of Re in the sample with $x=26$ and the external field dependence of the signal intensity at 1.3 K. The solid curve ρ shows the change in the electrical resistivity.

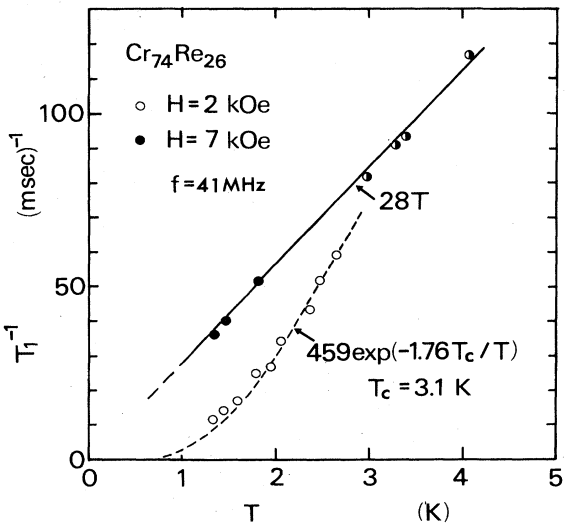

FIG. 6. Temperature dependence of the nuclear spin-lattice relaxation rate $1/T_1$ in the sample with $x=26$. The solid line shows the Korringa relation and the dashed curve the relaxation rate predicted by the BCS theory.

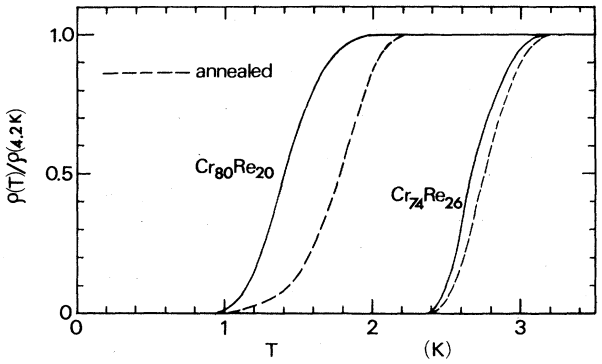

FIG. 7. Annealing effect of the relative resistivity change near the superconducting transition temperature for the samples with $x=20$ and $x=26$. The dashed curves show the resistivity changes of annealed samples.

C. Annealing effects

Annealing effects were measured for the samples with $x \leqq 30$ annealed at 1000 °C for 1 week. The crystal structure was bcc. Their lattice constants were little different from those of the unannealed alloy. The temperature dependence of resistivity near T_c is shown in Fig. 7 for annealed (solid line) and unannealed (dashed line) samples with $x=20$ and 26. The superconducting transition temperature increases by 0.1—0.5 K after the annealing. The width of the transition changes little with annealing in both samples.

Figure 8 shows plots of H_{C2} versus T for the sample with $x=26$. The upper critical field extrapolated to $T=0$ $[H_{C2}(0)]$ decreases from 5.9 to 4.4 kOe after annealing. The $H_{C2}(0)$ estimated from the weak-coupling formula is ~ 4.2 kOe with a resistivity of 7.5 μohm cm below 4.2 K. Since the electronic specific-heat coefficient

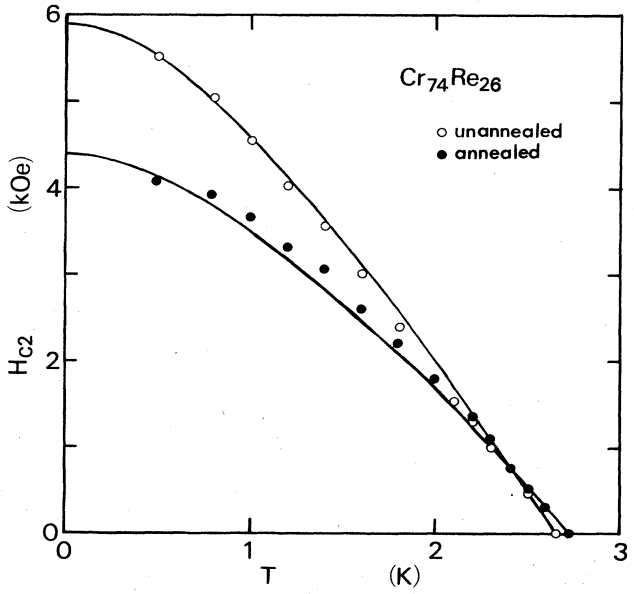

FIG. 8. Temperature dependence of H_{C2} in annealed and unannealed samples with $x=26$. Solid curves are calculated from the BCS theory in the dirty limit.

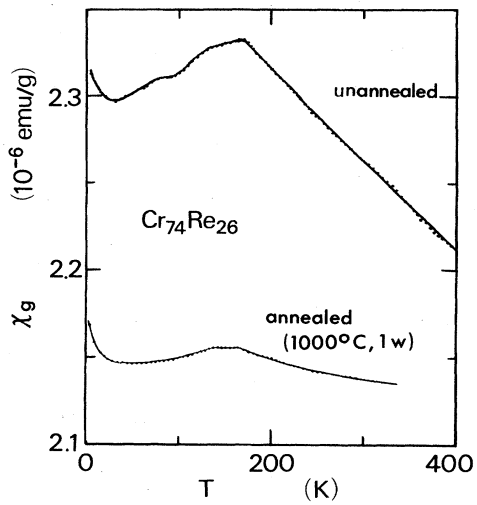

FIG. 9. Temperature dependence of the susceptibility of annealed and unannealed samples with $x=26$.

γ shows no change upon annealing,[6] the resistivity of the annealed sample is estimated from the change in $H_{C2}(0)$. The estimated value is ~ 0.7 times as large as that of the unannealed sample. The observed resistivity of the annealed sample is 0.82 ± 0.07 times that of the unannealed sample. The decrease in H_{C2} is explained by the increase in the mean free path of the electrons.

The susceptibility of the annealed sample decreases by 5—20% compared with that of the unannealed sample below 80 K. Both the variation with temperature and the peak around 160 K become small upon annealing, as shown in Fig. 9. However, a clear peak is still observed around 160 K in the annealed sample. Thus, we find that antiferromagnetic order remains in annealed alloys. In pure chromium the commensurate SDW is induced by strain and the Néel temperature in the strained state is larger than that in the annealed state.[17] In Cr-Re alloys the Néel temperature is insensitive to the strain. This might be a reflection of the fact that the SDW is commensurate both in strained and annealed Cr-Re alloys.

III. DISCUSSION

A. Coexistence of SDW and superconductivity

The temperature dependence of the susceptibility shows a peak around 160 K in both annealed and unannealed Cr-Re alloys with the Re concentration greater than 20 at. %. These alloys have a superconducting transition temperature of ~ 3 K. A magnetic hyperfine field of ~ 52 kOe was observed below 4.2 K at Re nuclei in the sample with $x=26$. It is clear that bcc Cr-Re alloys with the Re concentration greater than ~ 20 at. % are antiferromagnetic. The nuclear spin-lattice relaxation time of Re in the vortex state increases exponentially with decreasing temperature, as in the case of a BCS superconductor. These results indicate that antiferromagnetic order and superconductivity coexist not in different parts but in the same part of the sample.

To clarify the effect of magnetic ordering on the superconducting state, we compare the superconducting transition temperatures of Mo-Re and W-Re alloys[18,19] with those of Cr-Re alloys. Mo and W are 4*d* and 5*d* metals with the same number of valence electrons as Cr. However, their alloys with Re do not exhibit magnetic order. Figure 10 shows the Re-concentration dependence of the superconducting transition temperature in Cr-Re, Mo-Re, and W-Re alloys, normalized by the maximum transition temperature $T_c^{\max}$ near 40 at. % Re. The superconducting transition temperatures of bcc Mo-Re and W-Re alloys start to increase at ~ 10 at. % Re and saturate above ~ 25 at. % Re. The increase in T_c of Mo-Re and W-Re alloys correlates well with the change in the electronic specific-heat coefficient γ. In the Cr-Re system, the magnetic order becomes weak with increasing Re concentration over 30 at. %. Therefore, the rapid increase in T_c above 30 at. % Re may be attributed to the disappearance of the magnetic order. In other words, the difference in $T_c/T_c^{\max}$ between Cr-Re and other alloys is due to its suppression of superconductivity by itinerant electron antiferromagnetism.

The coexistence problem of SDW and superconductivity has been studied theoretically by Machida.[15] When a part of the Fermi surface satisfies the nesting condition and contributes to form the SDW state, the density of states (N_{E_F}) at the Fermi surface divides into two parts $N_{\rm SDW}$ and $N_{\rm SUPER}$. The SDW gap is formed using the $N_{\rm SDW}$ part of N_{E_F} and the superconducting gap in the rest ($N_{E_F}-N_{\rm SDW}=N_{\rm SUPER}$). Here, we write the superconducting transition temperature without SDW as T_{c0} and the magnetic transition temperature without superconductivity as T_{N0}. When $T_{N0}<T_{c0}$, the superconducting gap opens all over the Fermi surface and the SDW is completely suppressed. On the other hand, in case of $T_{N0}>T_{c0}$, the two types of long-range order generally coexist. The superconducting transition temperature in the presence of SDW is lower than T_{c0}. For $T_{N0}\gg T_{c0}$, the superconducting transition temperature T_c is given[15] as

$$T_c \sim T_{c0}(T_{c0}/2.7T_{N0})^{N_{\rm SDW}/N_{\rm SUPER}} . \quad (1)$$

In the CrRe system T_{N0} is ~ 160 K. T_{c0} is estimated from the superconducting transition temperature to be ~ 5.5 K near the Re concentration of 40 at. % where the magnetic order disappears. To obtain the observed T_c of ~ 3 K in the region of 20—30 at. % Re, $N_{\rm SDW}=0.12N_{E_F}$ is obtained from Eq. (1). In this system about 10% of the Fermi surface contributes to form the SDW state.

The concentration-dependent antiferromagnetic transition temperatures determined from the peak of the susceptibility and the superconducting transition temperature are summarized in Fig. 11. The magnetic transition temperature decreases sharply around 16 at. % Re from 580 K to 160 K, together with the onset of superconductivity. The lattice constant linearly increases with increasing Re concentration and shows no change around 16 at. % Re, as shown in Fig. 1. Therefore, it is evident that the lattice change is not the main origin of the changes in the magnetic and electrical properties around 16 at. % Re. It is likely that the shape of the Fermi surface alters around 16 at. % Re with increasing *d*-electron number and that only a part of the Fermi surface satisfies the nesting condition above 16 at. % Re. The superconducting state appears in the remaining part of the Fermi surface. In the lower

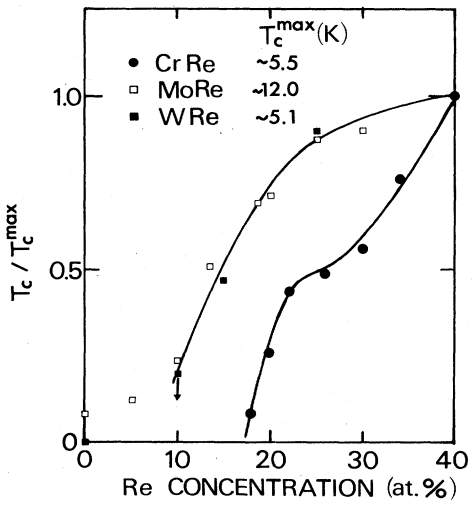

FIG. 10. Re-concentration dependence of superconducting transition temperatures normalized by the maximum transition temperature $T_c^{\max}$ in bcc Cr-Re, Mo-Re (Ref. 18), and W-Re (Ref. 19) alloys.

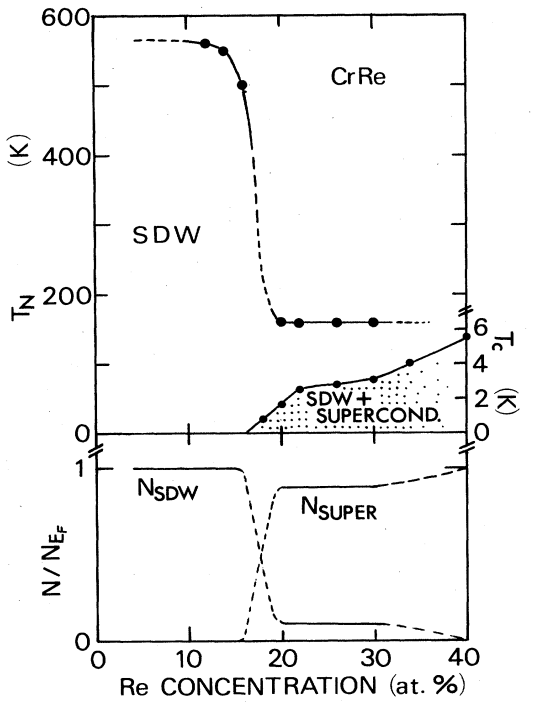

FIG. 11. Superconducting and antiferromagnetic transition temperatures of bcc Cr-Re alloys. The lower part shows the relative changes in the electron densities at the Fermi surface which contribute to spin-density waves ($N_{\rm SDW}$) and superconductivity ($N_{\rm SUPER}$). These values are estimated from the theory by Machida.[15]

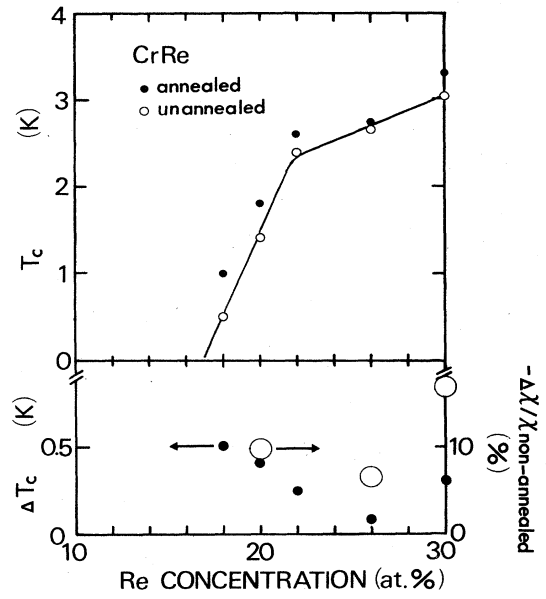

FIG. 12. Changes in the superconducting transition temperature upon annealing. The lower part shows the differences in the superconducting transition temperature and the susceptibility below 80 K between annealed and unannealed values.

part of the figure, the changes in the electron densities at the Fermi surface which contribute to the SDW state (N_{SDW}) and the superconducting state (N_{SUPER}) are shown schematically.

B. Competition between SDW and superconductivity

The superconducting transition temperature increases upon annealing, as shown in Fig. 12. This increase in the transition temperature is also reported by Muheim and Müller[6] for the Re-concentration range between 20 and 30 at. %. The electronic specific-heat coefficient γ and the Debye temperature show little change upon annealing.[6,20] On the other hand, the magnetic susceptibility decreases by $\sim 10\%$ of the unannealed value below ~ 80 K. The lower part of the figure shows the differences in the superconducting transition temperature and the susceptibility between annealed and unannealed values. The result suggests that the change in the transition temperature is correlated with the change in the magnetic state. The annealing relaxes the stress in the sample which induces magnetic moments, such as in pure Cr.[17] Thus, the decrease in the susceptibility can be explained from the decrease in magnetic densities induced by the stress.

Using Eq. (1) derived from the coexistence model of SDW and superconductivity, the increase in the superconducting transition temperature by ~ 0.3 K gives a change in the SDW density of $\Delta N_{SDW}/N_{SDW} \sim -0.2$. That is, the electron density at the Fermi surface which contributes to the SDW state decreases by $\sim 20\%$ of the unannealed value. This value is the same order as the observed decrease in the susceptibility upon annealing. Therefore, the increase in the superconducting transition temperature upon annealing is understood from the competing effect between SDW and superconductivity.

IV. CONCLUSION

The antiferromagnetic transition temperature of bcc Cr-Re alloys rapidly decreases around 16 at. % Re with increasing Re concentration. Corresponding to this change, superconductivity appears above this Re concentration. From the nuclear magnetic resonance of Re and susceptibility measurements, it is concluded that antiferromagnetic order remains above 16 at. % Re and coexists with superconductivity. The antiferromagnetic transition temperature is ~ 160 K above 20 at. % Re and is almost independent of Re concentration. The antiferromagnetic order is weak near 40 at. % Re. The superconducting transition temperature increases together with the disappearance of the magnetic order. Using the coexistence model of spin-density waves and superconductivity, we find that about 10% of the Fermi surface contributes to form the gap of the spin-density waves and the rest to form the superconducting gap in the Re concentration of 20—30 at. %. After annealing at 1000 °C, the superconducting transition temperature increases by 0.1—0.5 K and the susceptibility decreases by $\sim 10\%$ in the samples with $x \leq 30$. The result can be explained as arising from the competing effect of spin-density waves and superconductivity.

ACKNOWLEDGMENTS

The authors would like to thank Professor S. Ogawa and Professor K. Asayama for valuable discussions and Mr. S. Waki for experimental help.

[1]See, for example, *Superconductivity in Ternary Compounds II*, edited by M. B. Maple and Ø. Fisher (Springer, New York, 1982).
[2]B. V. B. Sarkissian, J. Appl. Phys. **53**, 8070 (1982).
[3]Y. Yamaguchi, Y. Nishihara, and S. Ogawa, J. Phys. Soc. Jpn. **53**, 3985 (1984).
[4]Y. Yamaguchi and Y. Nishihara, Solid State Commun. **50**, 785 (1984).
[5]R. P. Elliott, *Constitution of Binary Alloys, First Supplement* (McGraw-Hill, New York, 1965), p. 356.
[6]J. Muheim and J. Müller, Phys. Kondens. Mater. **2**, 377 (1964).
[7]J. G. Booth, Phys. Status Solidi **7**, K157 (1964).
[8]A. L. Trego and A. R. Mackintosh, Phys. Rev. **166**, 495 (1968).
[9]H. B. Møller, A. L. Trego, and A. R. Mackintosh, Solid State Commun. **3**, 137 (1965).
[10]W. C. Koehler, R. M. Moon, A. L. Trego, and A. R. Mackin-

tosh, Phys. Rev. **151**, 405 (1966).
[11]K. Mikke and J. Jankowska, J. Magn. Magn. Mater. **14**, 280 (1979).
[12]K. Mikke and J. Jankowska, J. Phys. F **10**, L159 (1980).
[13]Y. Nishihara, Y. Yamaguchi, S. Waki, and T. Kohara, J. Phys. Soc. Jpn. **52**, 2301 (1983).
[14]T. Kohara, K. Asayama, Y. Nishihara, and Y. Yamaguchi, Solid State Commun. **49**, 31 (1984).
[15]K. Machida, J. Phys. Soc. Jpn. **50**, 2195 (1981).
[16]D. Jérome, J. Magn. Magn. Mater. **31-34**, 20 (1983).
[17]G. E. Bacon and N. Cowlam, J. Phys. C **2**, 238 (1969).
[18]F. J. Morin and J. P. Maita, Phys. Rev. **129**, 1115 (1963).
[19]J. K. Hulm and R. D. Blaugher, Phys. Rev. **123**, 116 (1962).
[20]K. Takeda (private communication).